



# Geometric and aero-thermal influences on multiholed plate temperature: application on combustor wall

B. Leger<sup>a,\*</sup>, P. Miron<sup>a</sup>, J.M. Emidio<sup>b</sup>

<sup>a</sup> EA 1932: Laboratoire Aquitain de Recherche en Aérothermique, Université de Pau et des Pays de l'Adour, clo Turbomeca, 64 511 Bordes Cedex, France

<sup>b</sup> Service Aérothermodynamique, Société Turbomeca, 64 511 Bordes, France

Received 25 July 2002; received in revised form 22 August 2002

## Abstract

The increase in turbomachine performance implies the augmentation of pressures and working temperatures. Therefore, for the combustion chambers walls, high thermal stresses are involved. Thermomechanical metal properties require the improvement of parietal cooling methods. The multihole cooling method seems to present great potential and interest. By means of infrared thermography, we have studied the geometrical parameters and aero-thermal conditions to determine the optimal multiholed plate geometry, necessary in different combustion zones of combustor walls. For the same air consumption, we can obtain different cooling characteristics in terms of temperature gradient, efficiency and film cooling effect.

© 2002 Elsevier Science Ltd. All rights reserved.

**Keywords:** Film cooling effect; Multiholed plate geometry; Combustion chamber wall; Infrared thermography; Wall cooling effectiveness; Blowing rate

## 1. Introduction

To satisfy the growing interest in the increase of both compressor outlet and turbine entry temperatures, the properties of metal-alloys employed in gas turbine components and the methods for cooling them must be improved. There is little hope for a dramatic improvement in material properties, apart from the development of high-temperature ceramic components; thus, technology for cooling metal walls efficiently is required. Almost all current gas turbine engines employ the film cooling technique for combustor chamber wall cooling.

Film cooling requires approximately 40% of the total air mass flow rate coming from the compressor to produce combustion chamber exit gas temperatures of about 1500 K [1]. Thus, a very small air mass flow quantity would be left for combustion, which would be

highly unacceptable, especially for lean combustion processes or for fuels with low calorific values where a large proportion of the air is required for the combustion process. Multiholed walls in the combustion chamber remain a satisfactory, efficient and low-cost solution to the problem.

In our laboratory, we have designed a test cell, which allows us to improve our knowledge of this type of cooling technique by varying the aero-thermal and geometric parameters [2]. Many studies have been conducted on a single hole [3,4] or on one, two or three rows of holes [5,6]. These studies show the aerodynamic and thermal aspects of this kind of film cooling technique (jet penetration, turbulence analysis, the increase of local heat transfer in and around the hole, etc.). In most cases, applications for turbine vanes cooling systems are at issue, where the blowing rate [ $m = (\rho V)_{\text{jet}}/(\rho V)_{\text{h}}$ ] is low,  $m \sim 2$ , compared with big blowing rates encountered in multiholed combustor chamber walls, where  $m \sim 3$ –8.

Our experimental study concerns multiholed flat plates used in combustion chambers, at a scale of 1:1,

\* Corresponding author.

E-mail address: [bruno.leger@turbomeca.fr](mailto:bruno.leger@turbomeca.fr) (B. Leger).

### Nomenclature

$d$	hole diameter (m)
$e$	plate thickness (m)
$L$	multiholed zone length (m)
$m$	blowing ratio = $(\rho V)_{\text{jet}}/(\rho V)_h$
$Ma$	Mach number
$p$	inter-row streamwise distance (m)
$P$	pressure (Pa)
$Rfc$	flow ratio
$s$	inter-row longitudinal distance (m)
$T$	temperature (K)
UI	infrared unity
$V$	velocity (m/s)
$x$	distance, length (m)

### Greek symbols

$\alpha$	hole angle inclination ( $^\circ$ )
$\Delta P$	pressure drop
$\varepsilon$	plate emissivity

$\eta_w$	wall cooling effectiveness (%)
$\rho_{h,c}$	hot and cold air density ( $\text{kg/m}^3$ )
$\tau$	transmissivity

### Subscripts

atm	atmospheric
c	cold
C	casing
ext	exterior
h	hot
jet	inside holes
PH	port hole
pl	plate
ref	reference
w	wall

### Superscripts

$^\circ$	black body
*	dimensionless parameter

tested in realistic aerodynamic and thermal environment conditions. Many investigations about multihole cooling systems have been carried out, but much of the work was aimed at different scales [7], lower temperature levels or used a different air supply method for multiholed walls [8,9]. In our case, the cold flow does not completely pass through the holes (see Fig. 1), which corresponds exactly to the real cold air flow type existing in combustion chambers.

We have carried out a number of tests in order to determine the influence of geometric parameters on the multiholed wall cooling process. Fig. 2 shows the geometric configuration of the multiholed plate. Experiments were conducted on 8 different geometry plates, selected in order to explore the influence of geometric

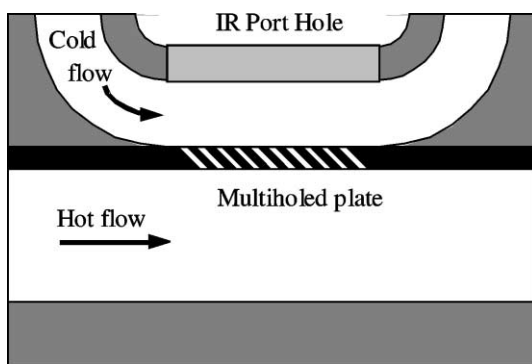


Fig. 1. Schematic of the air flows on the multiholed plate bench.

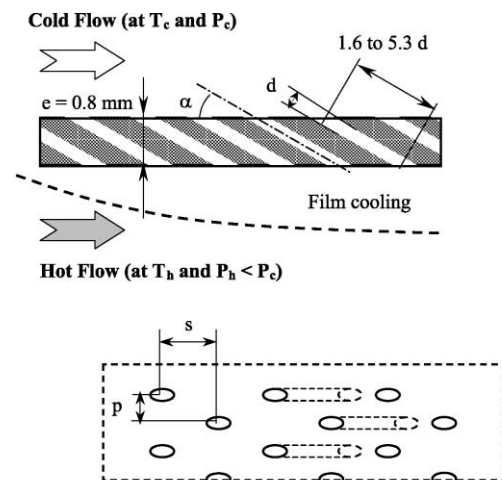


Fig. 2. Geometrical configuration of the multiholed plate.

parameters on the plate temperature. Table 1 gives the tested geometric parameter range.

For each plate, we have studied 32 specific aero-thermal conditions, selected in order to investigate a large range of aero-thermal conditions encountered in gas turbine combustion chambers. Table 2 shows the entire range of aero-thermal conditions tested.

## 2. Experimental investigations

Plate surface temperature is measured on the cold side, using an infrared camera system. The infrared

Table 1  
Geometric parameters

$\alpha^\circ$	20–150
$d$ (mm)	0.3–0.7
$p$ (mm)	1.025–1.685
$s$ (mm)	0.905–4.03
$L$ (mm)	23.36–99.28

Table 2  
Aero-thermal tested conditions

$\Delta P/P$ (%)	$T_h$ (K)	$V_c$ (m/s)	$V_h$ (m/s)	$P$ (Pa)
0.5–12	860–1400	27–80	34–102	101325

camera receives an analogue signal ( $UI_{pl}$ ) proportional to the radiation given off by the plate (Fig. 3). This raw signal contains the real emission of the plate ( $\epsilon_{pl}UI_{pl}^\circ$ ), the reflected radiation of casing walls around the plate ( $(1 - \epsilon_{pl})UI_C^\circ$ ), and the interfered radiation ( $UI_{ext}^\circ$ ). If  $UI_{pl}$  is the radiometric flux measured by the infrared camera in infrared units, we can write:

$$UI_{pl} = \tau_{atm}\tau_{PH}\epsilon_{pl}UI_{pl}^\circ + \tau_{atm}\tau_{PH}(1 - \epsilon_{pl})UI_C^\circ + \tau_{atm}(1 - \tau_{PH} - \rho_{PH})UI_{PH}^\circ + \tau_{atm}^2\rho_{PH}UI_{ext}^\circ$$

The aim of the measuring process is to eliminate interference and to calculate the plate temperature levels  $U^\circ(T_{pl})$  referring to a black body.

The plate is considered very thin (the Biot number is smaller than 0.1) and we calculate the plate temperature with a self-developed code. In order to determine the true temperature of the multiholed plate, according to our experimental conditions, it is necessary that each thermal picture pass through a classic IR camera filtering process [10]:

- noise filtering process—eliminate the raw signal exterior interference;
- deconvolution and radiation filtering process—identify and eliminate the noise radiation coming from the hot side through holes;
- spatial filtering—to respect the spatial resolution of the infrared camera;
- determining the raw wall temperature—using Planck’s law.

After all these processes, we can determine the multiholed plate temperature ( $T_{pl}$ ). We have to mention here that the plate emissivity ( $\epsilon_{pl}$ ) has been separately measured on a special reflectometer test bench by CEA at Bordeaux, France.

### 3. Results

Several multiholed plates have been designed and tested to determine the influence of geometric parameters on the wall temperature and cooling effectiveness. This section provides examples of results achieved within the present study.

#### 3.1. Multiholed plate temperature

For the multiholed plate cooling technique we can identify three different zones, as in Fig. 4.

- “Upstream zone”—located before the multiholed zone; here the heat transfer is made by conduction through and along the plate and also by convection and radiation on both sides of the plate.
- “Multiholed zone”—in this zone the heat transfer is made by convection, conduction through holes, radiation and by the film cooling effect.
- “Downstream zone”—situated after the multiholed zone, it is here that the film cooling effect is developed and achieved.

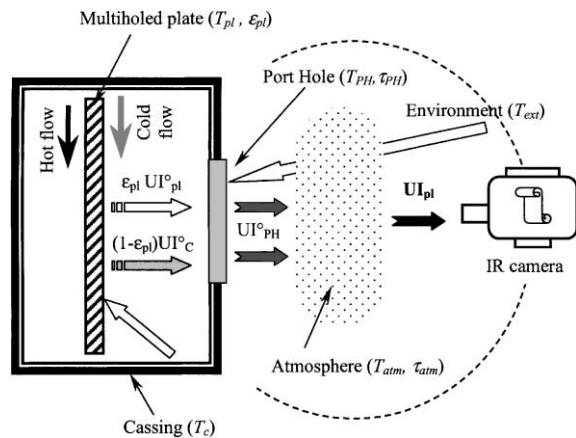


Fig. 3. Components of IR measured signal.

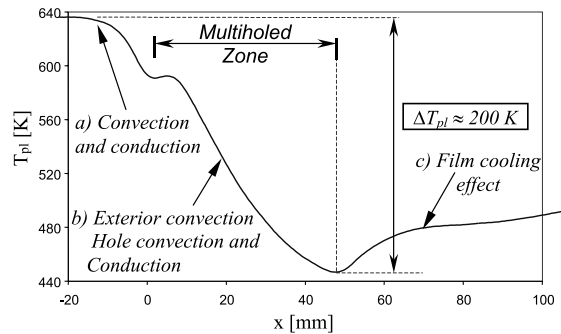


Fig. 4. Heat transfer for the multiholed test plate.

We can understand why this kind of cooling technique is interesting: the wall temperature drops from 640 K to 440 K along a 50 mm multiholed zone. In the downstream zone, we obtain a film cooling effect, which maintains a low wall temperature ( $\sim 480$  K) for about 70 mm after the last row of holes, and this is done without any supplementary air consumption.

### 3.2. Wall cooling effectiveness

The multiholed zone of the plate leads to a large decrease in plate temperature. This decreasing temperature effect is due to the increasing convective heat transfer inside the holes and, also, to the creation of a film cooling effect on the hot side of the plate (see Fig. 4). The convective heat transfer process in the holes depends on the heat transfer coefficient, the interior hole surface and the air flow temperature. The geometrical parameters have a direct influence on the surface hole and on the cold air velocity through the holes. By modifying the geometrical parameters, it is possible to obtain the necessary convective heat transfer with a minimum air cold flow. The film cooling has to be stable to avoid the mixing between the cold air issued from the holes and the hot main flow of the combustor chamber as much as possible. In the following, we analyse the influence of both geometrical and aero-thermal parameters on plate temperature.

We introduce  $\eta_w$ , called the wall cooling effectiveness, which describes the efficiency of multiholed plate cooling:

$$\eta_w = (T_h - T_{pl}) / (T_h - T_c)$$

We have obtained a set of different graphs showing the development of the wall cooling effectiveness for all the plates tested in all aero-thermal conditions. Then we studied the influence of each geometrical and aero-thermal parameters on the wall cooling effectiveness ( $\eta_w$ ) separately.

The cooling efficiency value in the upstream zone of the multiholed plate is the same as the cooling efficiency value of a simple plain plate ( $\eta_w \sim 0.79$ ). However, here the heat transfer is done only by convection on both sides of the plate. For the downstream zone, the cooling effectiveness value is increased,  $\eta_w = 0.88$  and a film cooling effect is created and maintained along the plate, after the multihole zone (see Fig. 5). At the beginning of the multiholed zone, a minimum cooling efficiency value is attained. This anomaly is explained by a combination of both aero-thermal and geometric parameters. This strange combination has to be made known and avoided. The multiholed plate cooling efficiency is increased by 15% compared to a normal plain plate without holes. This is due to convection through holes and to the creation of a cold film along the plate on the hot side.

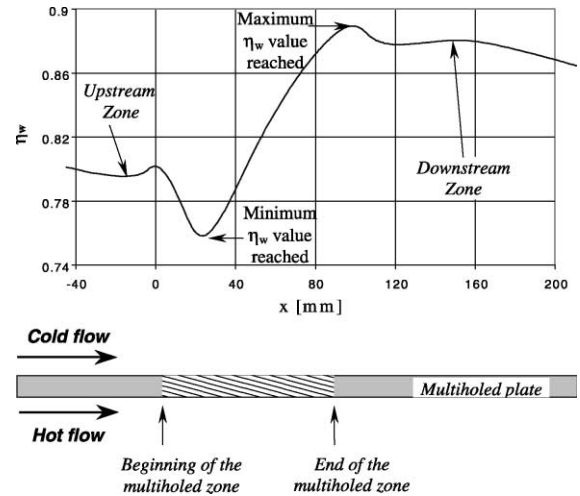


Fig. 5. Particular zones in cooling efficiency evolution of multiholed plate.

In the next paragraphs, all geometrical and aero-thermal dimensionless parameters (marked with \* superscript) refer to standard aero-thermal conditions tested on a reference plate of our laboratory. The reference plate has the following geometrical characteristics:

$$\alpha_{\text{ref}} = 30^\circ; \quad d_{\text{ref}} = 0.5 \text{ mm}; \quad L_{\text{ref}} = 49.64 \text{ mm}; \\ p_{\text{ref}} = 3.37 \text{ mm}; \quad s_{\text{ref}} = 2.92 \text{ mm}$$

The standard aero-thermal conditions are:

$$(\rho_c V_c)_{\text{ref}} = 54.17 \text{ kg m}^{-2} \text{ s}^{-1}; \\ (\rho_h V_h)_{\text{ref}} = 17.71 \text{ kg m}^{-2} \text{ s}^{-1}; \\ (T_h/T_c)_{\text{ref}} = 3.87 \quad \text{and} \quad \Delta P_{\text{ref}} = (P_c - P_h)/P_c = 4.80\%$$

#### 3.2.1. Influence of the multiholed zone length on the wall cooling effectiveness

We compared the plate with a reference multiholed zone length,  $L^* = 1$  and another plate with  $L^* = 1.59$ , in the same aero-thermal conditions (as in Fig. 6).

For both plates, between  $x = 0$  and 80 mm, the rise in the cooling efficiency increases from 0.67 to 0.81. But for the second plate, with a double multiholed zone length ( $L_2^*$ ), into the downstream zone, at  $x = 150$  mm, the cooling efficiency is 8% higher than the cooling efficiency of the first plate at the same co-ordinate.

But this 8% rise in the cooling efficiency leads to a double mass cold air consumption. So we can say that there is a minimum multiholed zone length, necessary to obtain an optimal wall cooling efficiency; this minimum length of the multiholed zone depends on the existing aero-thermal conditions and the imposed temperature level to be expected.

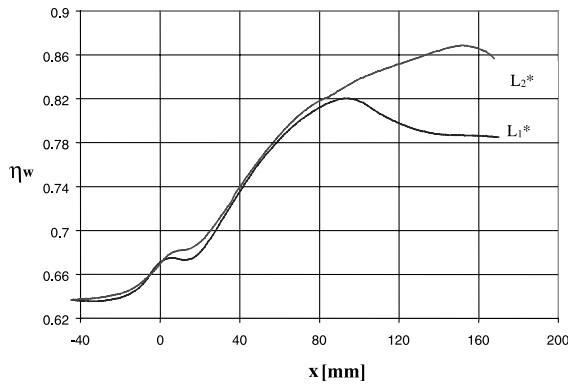


Fig. 6. Influence of multiholed zone length on the wall cooling effectiveness.

3.2.2. Influence of hole angle inclination ( $\alpha$ ) on the wall cooling effectiveness

In the same aero-thermal conditions and at the same level of air consumption, we compared the plates with  $\alpha = 30, 90$  and  $150^\circ$  hole angle inclination (Fig. 7). Between  $x = 0$  and  $100$  mm the wall cooling effectiveness is approximately the same for both plates  $\alpha = 30^\circ$  and  $90^\circ$ . At  $x = 100$  mm the cooling efficiency of  $\alpha = 90^\circ$  plate is 4% smaller than the efficiency of the  $\alpha = 30^\circ$  plate. Also, in the downstream zone, at  $x = 160$  mm, the wall cooling effectiveness of  $\alpha = 30^\circ$  plate is greater than the wall cooling effectiveness for the plate with  $\alpha = 90^\circ$ . In the case of the  $\alpha = 30^\circ$  plate the cold film is closer to the wall and has a better cooling efficiency. In the case of the  $\alpha = 150^\circ$  plate, cold flow direction passing through holes is reversed. This fact completely changes the development of wall cooling effectiveness. In this case, only 30% of the  $\alpha = 30^\circ$  plate length is required in order to obtain the same maximal cooling efficiency value. But this involves the presence of an elevated temperature gradient in the multiholed zone, which is dangerous for the plate thermal resistance. For the downstream zone of

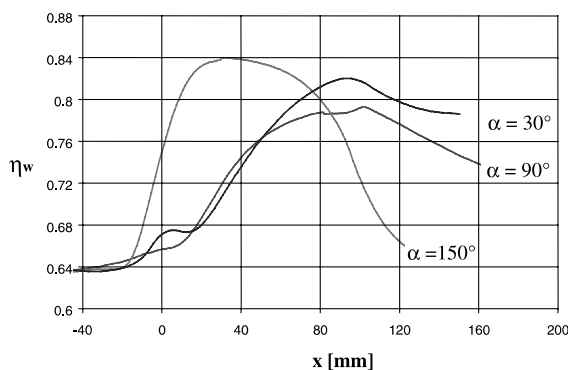


Fig. 7. Influence of hole angle inclination on the wall cooling effectiveness.

$\alpha = 150^\circ$  plate, the film cooling effect is not present anymore. The injected cold air does not create a film along the plate; it just mixes very quickly with the hot gases.

3.2.3. Influence of the hole diameter ( $d$ ) on the wall cooling effectiveness

For the same aero-thermal conditions, the reference plate with  $d^* = 1$  and a second plate with  $d^* = 1.4$  are compared in Fig. 8. Increasing the hole diameter, the passage hole surface section is multiplied by 2.12. The result is a 5% cooling efficiency rise and also a large reduction in the aero-thermal anomaly effect at the beginning of the multiholed zone.

3.2.4. Influence of the inter-row distance ( $s$ ) on the wall cooling effectiveness

In Fig. 9, the plate with  $s^* = 1$  and a second plate with  $s^* = 0.62$  are compared. In order to reduce the inter-row distance ( $s^* = 0.62$ ), we have chosen a plate with a smaller hole diameter ( $d^* = 0.6$ ). The best wall cooling effectiveness values are obtained for small inter-row distance values. The aero-thermal anomaly effect, for the first row of holes, is completely eliminated; instead, the cold mass air consumption is increased. We have established that for the same air consumption, we can obtain different cooling characteristics in terms of temperature gradient, cooling efficiency and film cooling effect, just by modifying the geometric parameters of the multiholed plate. In conclusion, we can choose the right multiholed plate geometry in order to obtain the wall cooling efficiency desired with minimum mass cold air consumption.

3.3. Aero-thermal conditions

The combustion process in the combustor gas turbine engines determines the aero-thermal conditions. These conditions are variable and depend on different zone of

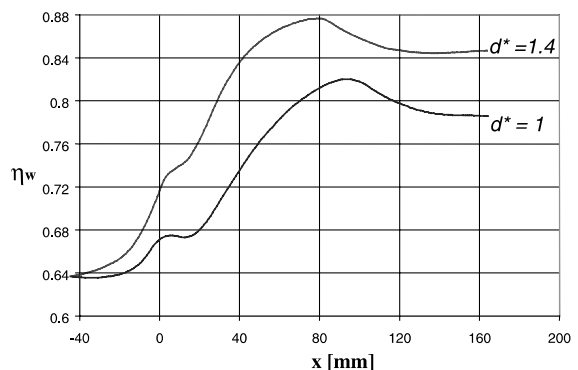


Fig. 8. Influence of hole diameter on the wall cooling effectiveness.

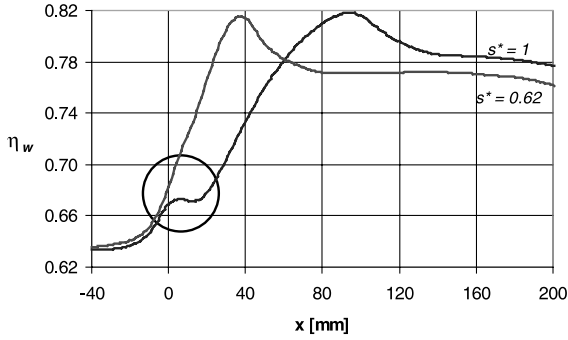


Fig. 9. Influence of inter-row distance on the wall cooling effectiveness.

the combustion chamber (primary zone, principal zone and dilution zone). So, we have studied the evolution of the wall cooling effectiveness for some aero-thermal conditions, in order to determine and adapt the geometry of the multiholed plates for different combustion zones in the combustion chambers.

3.3.1. Influence of the flow ratio ( $Rfc^*$ ) on the wall cooling effectiveness

$$Rfc^* = (\rho_c V_c) / (\rho_h V_h)$$

In Fig. 10, the flow ratio varies from 0.42 to 3.14, and is obtained by modifying the hot and cold velocities; the density  $\rho_c$  and  $\rho_h$  are supposed to be constant ( $Ma < 0.1$ ). For big flow ratio numbers ( $Rfc^* \sim 3$ ), the cold flow is much greater and the film cooling effect in the downstream zone is more effective (by 15%). But, with the same air consumption, better results for the

cooling efficiency are obtained at low flow ratio numbers.

3.3.2. Influence of the temperature ( $T$ ) on the wall cooling effectiveness

Temperature ratio  $[T_h/T_c]^*$  ranges between 0.9 and 1.25, but in fact only  $T_h$  varies from 860 to 1400 K,  $T_c = 300$  K is constant, see Fig. 11.

The maximum wall cooling effectiveness value drops from 0.86 to 0.82 when the temperature ratio rises. The development of cooling efficiency is approximately the same for all temperature ratios tested.

3.3.3. Influence of drop in pressure ( $\Delta P$ ) on the wall cooling effectiveness

$\Delta P = (P_c - P_h) / P_c$  is the pressure drop through the holes, between the cold side and the hot side of the plate. In Fig. 12, the  $\Delta P^*$  pressure drop tested varies from 0.66

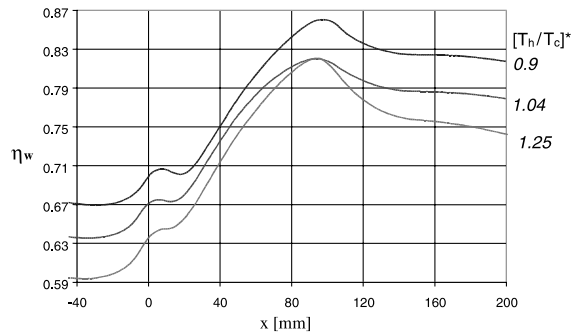


Fig. 11. Influence of temperature on the wall cooling effectiveness.

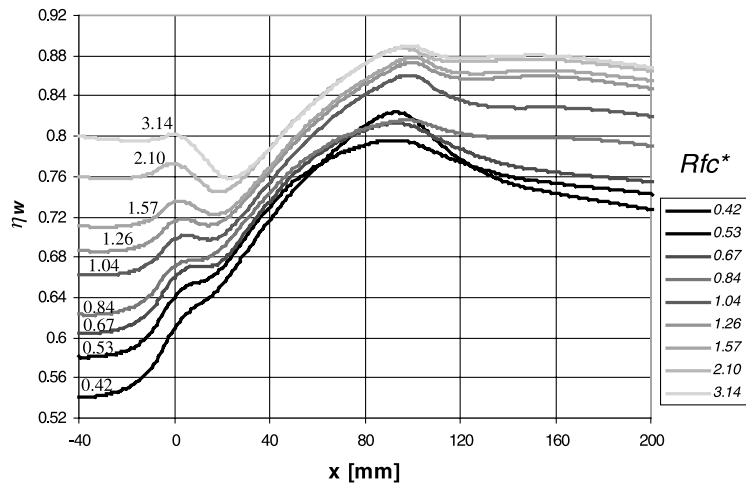


Fig. 10. Influence of flow ratio on the wall cooling effectiveness.

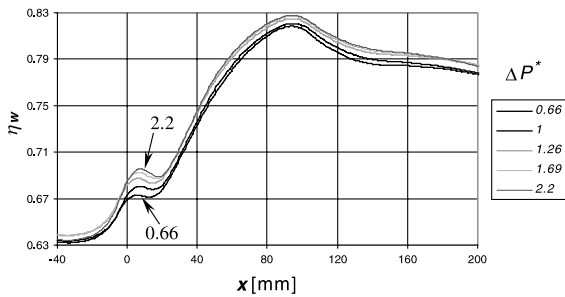


Fig. 12. Influence of drop in pressure on the wall cooling effectiveness.

to 2.2. For all zones of the multiholed plate, we can see that the wall cooling effectiveness does not increase too much, while  $\Delta P^*$  values increase greatly. So, for this kind of cooling technique, there is no need to have large drops in pressure. If  $\Delta P^*$  increases, the cooling air consumption also increases, but no gain in cooling effectiveness is obtained. We think that the film cooling along the plate is already strong enough and does not need to be fed with cold air anymore. Our aim is to reduce the cold flow air consumption which is used in the multiholed plate cooling process to a minimum, as far as is possible.

#### 4. Conclusions

We designed a test bench in our laboratory to study the multiholed cooling devices which are used in gas turbine combustion chambers. Our devices have a 1:1 scale and are tested in realistic aero-thermal conditions. The test cell is provided on the cold side of the multiholed plate with a port hole, permitting us to have a great deal of optical access, which is necessary to measure the plate temperature by means of an infra red camera. Numerous multiholed plates have been designed by varying the geometrical parameters such as hole diameter, hole angle inclination and hole pitches. All plates were tested in a large range of aero-thermal conditions. Each geometric and aero-thermal parameter has been separately studied in order to determine the influences on the plate temperature expressed here in terms of wall cooling effectiveness.

We have established that some geometric parameters such as multiholed zone length, hole angle inclination and hole diameter have a strong influence on the wall cooling efficiency and also on the cold air consumption necessary for plate cooling. For example, if the hole angle inclination ( $\alpha$ ) is too high, the film cooling effect created on the hot side of the plate will not be efficient because the cold air will immediately mix with the hot main stream. The hole diameter ( $d$ ) must be increased to

obtain a better wall cooling efficiency, but not too much so that the cold mass air consumption is kept to a minimum value. The multiholed zone length ( $L$ ) must be long enough to create a film cooling effect.

The multiholed geometry device must be chosen in order to obtain the temperature level desired with minimum cold air consumption. In a gas turbine combustor, the combustion process determines the thermal conditions on the combustor walls. To take these conditions into account in the cooling devices, we are using different multiholed geometry for each different combustor wall zone. From the same air flow consumption we can obtain different cooling characteristics in terms of temperature gradient, wall cooling efficiency and film cooling effect, downstream the multiholed zone.

The aim of this study is to make a database available to design the right multiholed geometry in order to optimise the wall cooling process in gas turbine combustors. The optimisation process consists in finding the good compromise between the cold air consumption and the wall temperature levels reached whatever the aero-thermal conditions may be.

There are now two ways of conducting new investigations: the first consists in using different hole diameters for the same multiholed plate zone, larger diameters at the beginning of the multiholed zone and smaller at the end, in order to keep the cooling film close to the plate.

The second way is to use two or three much smaller different multiholed zones on the same plate. The film cooling effect created after a multiholed zone protects the plate for quite a significant distance in the downstream zone, so it is not necessary to create holes along the entire plate surface.

These two ways of investigations are now tested in our laboratory and we are expecting to obtain more of a reduction in the cold mass air consumption for the combustion chamber walls cooling system.

#### References

- [1] G.E. Andrews, M.C. Mkpadi, Full-coverage discrete hole wall cooling: discharge coefficients, *J. Eng. Gas Turbines Power* 106 (1984) 183.
- [2] B. Leger, P. Andre, G. Grienne, G. Schott, Contrôle thermique de parois de chambre de combustion. Banc d'essai du Laboratoire Aquitain de Recherche en Aérothermique, *Revue générale de thermique* 35 (1996) 625.
- [3] E. Le Grives, J.J. Nicolas, J. Genot, Internal Aerodynamics and heat transfer problem associated to film cooling of gas turbines, ASME no. 79, GT 57, 1979.
- [4] T.F. Fric, A. Roshko, Vortical structures in the wake of a transverse jet, *J. Fluid Mech.* 279 (1994) 1–47.
- [5] A. Brown, C.L. Saluja, Film cooling from three rows of holes on adiabatic constant heat flux and isothermal surfaces in the presence of variable freestream velocity

- gradient and turbulence intensity, ASME no. 79, GT 24, 1979.
- [6] R.J. Goldstein, Effect of mainstream variables on jets issuing from a row of inclined round holes, *J. Eng. Power* 101 (1979) 289–304.
- [7] J. Descoins, Caractérisation de techniques de refroidissement de paroi: Application de la thermographie infrarouge au cas du soufflage pariétal, Thèse de l'Ecole Nationale Supérieure de l'Aéronautique et de l'Espace, 1991.
- [8] J.L. Champion, E. Dorignac, B. Deshaies, Etude expérimentale du processus de refroidissement d'une plaque multiperforée, Congrès sur la thermique de l'homme et de son proche environnement, Société Française des Thermiciens, May 1995, pp. 254–259.
- [9] M. Martiny, A. Schultz, S. Wittig, Mathematical model describing the coupled heat transfer in effusion cooled combustor wall, ASME no. 97, GT 329, June 1997.
- [10] G. Gaussorgues, La thermographie infrarouge, Troisième édition Technique et Documentation—Lavoisier, 1989.